Resistance jumps and the nature of the finite-flux normal phase in ultra-thin superconducting cylinders

G.J. Conduit and Yigal Meir

Department of Physics, Ben Gurion University, Beer Sheva 84105, Israel

(Dated: June 6, 2011)

Recent observations have revealed the emergence of an unusual normal phase when a magnetic flux threads an ultra-thin superconducting cylinder. Moreover, with increasing temperature, the resistance rises in a series of abrupt jumps. These phenomena are explained using a novel approach, which allows calculation of the resistance in the presence of amplitude and phase fluctuations of the superconducting order parameter, and at the same time introduces a local probe of the current and chemical potential. It is demonstrated that phase fluctuations lead to the sequential breakdown of local superconducting phase correlations, resulting in the formation of normal weak links, which give rise to the emergence of the normal phase is a stepwise manner. Finally, specific predictions are made on how the experimental observations change with the cylinder geometry.

Almost half a century ago, Little and Parks [1] performed one of classic experiments in superconductivity: they demonstrated that the critical temperature of a cylindrical superconductor (SCR) varies periodically with the magnetic flux Φ threading the cylinder; the period $\Phi_0 \equiv hc/2e$ reflects the charge $2e$ of the Cooper pairs. This effect is well understood within the BCS mean-field model [2], as the kinetic energy of the electrons depends periodically on the magnetic flux. In fact, it has been predicted [3] and subsequently observed [4] that if the cylinder circumference is reduced to the same order as the SCR coherence length, the flux can drive the SCR into its normal phase even at the lowest temperature. Surprisingly [4], the resistance of this low-temperature normal phase, only weakly dependent on temperature, is considerably smaller than the high temperature, normal state resistance of that same sample. A subsequent experiment has revealed even more intriguing results: the resistance increased with rising temperature in a series of steps [5], which broadened with applied magnetic flux. The origin of these steps, and the nature of the resistive state at finite flux have become a subject of much debate. Originally it was suggested [5] that the steps arise due to consecutive events of phase separation in the vicinity of a quantum phase transition (see also [6]). It was later demonstrated [7, 8], however, that such a scenario is inconsistent with the system parameters, and a spontaneous transition to a symmetry broken order parameter is not possible. Alternatively, a mean-field-like calculation [7, 8] suggested that the observation might be due to disorder induced fluctuations in the coherence length. However, it was then claimed [9] that the large variation in the coherence length necessary to explain the data was inconsistent with other features in the experiments. Thus, the experimental observations remain hitherto unexplained.

In a two-dimensional system at the critical temperature T_{KT} phase fluctuations of the pairing amplitude drive vortices and anti-vortices to unbind and proliferate through the system [10]. The destruction of global phase coherence drives the loss of perfect conductance [11]. It is therefore imperative for any theory that attempts to describe the loss of superconductivity in these ultra-thin cylinders to take phase fluctuations into account. In this letter we utilize a new formulation [12] of transport through low-dimensional, possibly disordered SCRs (attached to two metallic leads), in the presence of finite temperature and magnetic field, to study a microscopic model of the Little-Parks effect. This *ab initio* tool, which employs an exact formula for the current, takes full account of thermal phase fluctuations of the superconducting (SC) order parameter, while neglecting its quantum fluctuations. This method has already been shown [12] to reproduce, for example, the classic Little-Parks effect and the conductance characteristics near the Kosterlitz-Thouless transition. Moreover, the new tool introduces a local probe of the normal and SC current and chemical potential distribution within the sample, giving us the opportunity to expose and understand the local physical processes that drive the loss of superconductivity and concomitant steps in the resistance. In the present case the intermediate region, an ultra-thin cylinder, sandwiched between two metallic leads, is described by the disordered negative-U Hubbard lattice model. The parameters that characterize the model, in addition to temperature T and magnetic flux Φ, are the on-site attraction U (all energies are expressed in terms of t, the uniform hopping integral), the typical disorder W – the width of the distribution of the on-site energies, and the average density n (see [12] for more details). The coupling between the noninteracting leads and the central region results in a length independent contact resistance, which can be easily dealt with. The magnetic field is applied parallel to the axis of the cylinder, which has a finite wall thickness d and inside radius r (expressed in terms of the lattice constant a).

Our strategy to study the Little-Parks effect in an ultra-thin cylinder is to first establish the geometry and key parameters required to recover the main experimental phenomena, and then compare and contrast the obser-
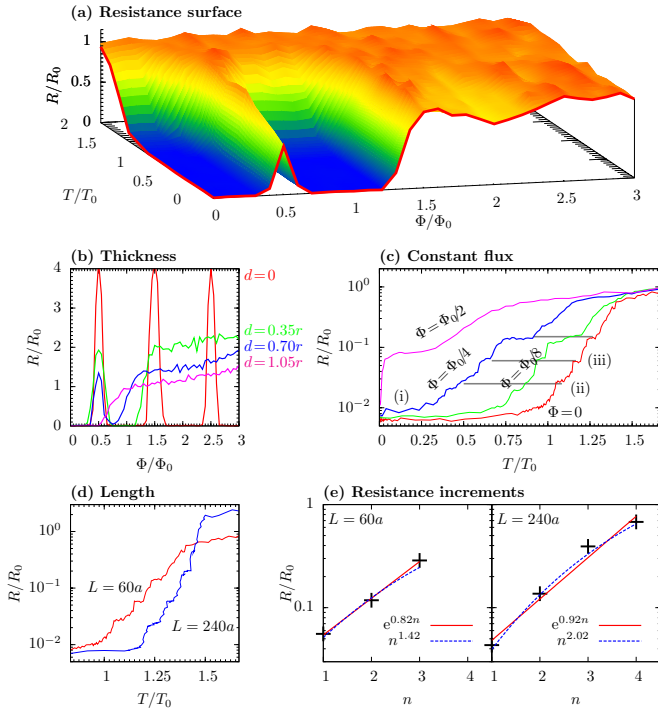
FIG. 1: (Color online) (a) The variation of resistance with flux Φ and temperature T, with the normal state at $\Phi = 0$ first emerging at temperature $T_0 = 0.11t$. $R_0 = 17h/e^2$ is the normal state resistance. The plot is perfectly symmetric in magnetic flux. (b) The variation of resistance with flux for four different cylinder wall thicknesses d. (c) Cuts through the resistance surface at four different magnetic fluxes. The horizontal gray lines denote the emergence of the first three steps. (d) Cuts through the resistance surface at zero flux for two different length SCRs. (e) The steps in the resistance against step number for systems of length $60a$ and $240a$ at $\Phi = 0$.

vations to experiment. Secondly, we will take advantage of our new capability to study the microscopic observables to highlight the underlying mechanisms that drive the emergence of the normal state. Finally, we will use our formalism to make predictions about further observable phenomena that could verify the validity of our approach and help pin down the nature of the transition.

In order to determine a suitable geometry for our cylinder, we first note that the resistance was not a periodic function of the magnetic field because of flux penetrating through the sample walls [4, 5]. Our first numerical results in Fig. 1(b) depict the magnetic field dependence of the resistance R for several wall thicknesses d. We find that the choice $d \approx 0.35r$ (which falls within the typical range of the experimental devices), has a reasonable resemblance to the experimental results, and the numerical results presented hereafter are for that choice of thickness (in all the calculations presented in this Letter, we set the parameters $U = 1.6t$, $W = 0.1t$, $n = 0.9$, use a cylinder of circumference $11a$, and length $L = 60a$). Fig. 1(a) depicts the dependence of the resistance with

flux and temperature. In addition to the expected suppression of superconductivity by temperature, it demonstrates the emergence of the normal phase at low temperature around $\Phi \approx \Phi_0/2$, and the recurrence of the SC phase for $\Phi_0/2 < \Phi < \Phi_0$. This surface displays the same qualitative features as the experimental results in Ref. [4]. In Fig. 1(c) we plot cuts through the surface at constant threading flux. The cut taken at zero flux contains a substantial SC phase region (where the resistance is only due to the contact resistance to the leads) before the resistance increases into the normal phase in a series of steps. Increasing flux lowers the transition temperature, until at half-integer flux the system starts out in a normal phase whose resistance then increases further with rising temperature. This normal state persists to almost $T = 0$ at which point the weakly coupled superconducting (SC) regions become phase locked and the resistance rapidly drops. This can also possibly be seen in some of the experimental results [5].

Having outlined the main qualitative behavior we now focus more closely on the emergence of the steps in the resistance, which are also seen in the experimental results [5]. For the cuts at different fluxes in Fig. 1(c), the steps in the resistance emerge at similar values of the overall resistance roughly independent of flux. Interestingly, for the longer $L = 240a$ wire shown in Fig. 1(d) more steps emerge. To examine these steps in more detail, Fig. 1(e) depicts the dependence of the resistance step value on the step number, for cylinders of two different lengths, $L = 60a$ and $L = 240a$. To reliably distinguish the steps we focus on only the lowest steps (these steps can be also positively identified from the successive emergence of boundaries in the phase coherence plots in the lower panel of Fig. 2, see below). The resistance steps are consistent with either an exponential (as deduced in the experimental paper [5]) or power law dependence.

Having reproduced the experimental results, we now take advantage of our ability to produce local current and voltage maps, and differentiate between SC (Cooperpair) and normal current [12], to expose the microscopic mechanism that leads to the emergence of the normal phase with increasing temperature and flux. We start at low temperature [point (i) in Fig. 1(c)] well below T_0, where the system first assumes a finite resistance. Here, as we can see in the current map, [top panel of Fig. 2(i)] all the current is SC. This conclusion is substantiated by the SC order parameter (second panel) being nearly constant along the wire. Defining the phase of the order parameter θ_x at a point x along the cylinder averaged over the circumference, we can see in the lower panel that the long-range SC correlation function $\langle \cos(\theta_{x1} - \theta_{x2}) \rangle$ is constant across the system, demonstrating that the entire SCR is phase coherent. We also note (third panel) that there are no vortices in the superconductor, and there is no voltage drop along the sample (fourth panel), so the only source of resistance is the contact resistance.

As temperature increases to $T = 1.2T_0$, [Fig. 2(ii), second panel, corresponding to point (ii) in Fig. 1(b)], the
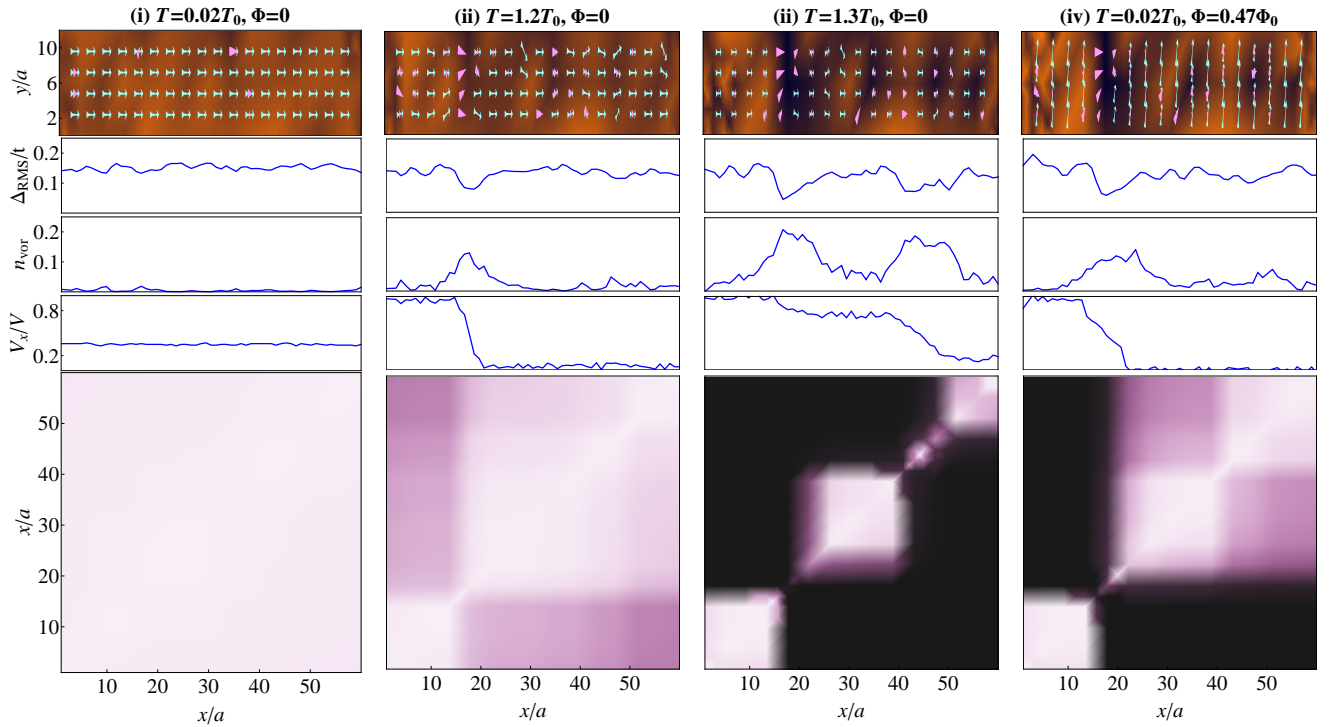
FIG. 2: (Color online) The current maps (upper) at four points labeled in Fig. 1(e). The normal current is shown by cyan pointers and supercurrent in magenta darts, whose length and direction reflects the local current flow. The map overlays the spatial variation of $|\Delta|$ shown by dark orange. The second row of plots show the column averaged variation of $|\Delta|$, the third row the column averaged number of vortices per site, and the fourth row the local potential. The bottom row shows the column averaged correlation $\langle \cos(\theta_{x1} - \theta_{x2}) \rangle$, with strong correlations in white, and weak in black.

SC correlations slightly weaken at around $x/a \simeq 17$ for this specific realization of disorder. While a mean-field calculation would still lead to long-range coherence in the sample, temperature also enhances phase fluctuations across the weaker SC region. These weaker local SC correlations allow nucleation of vortices at lower energy (see Fig. 2(ii) central panel) driving a local loss of correlation across the junction. This can be seen in the lower panel, where the system separates into two disconnected strongly correlated SC regions, giving rise to an effective Josephson junction, and a finite voltage developing across the junction (fourth panel). At this temperature the resistance effectively jumps to a finite value. The current through the system is naturally reduced, and in fact changes its character from SC to normal and back to SC as it crosses the junction (top panel). The bottom panel of Fig. 2(ii) indicates also that weaker correlations are developing between the two sides of $x/a \simeq 45$, which can be thought of as an effective Josephson junction whose maximal current is still larger than the current in the system, and thus no voltage drops across it. As temperature increases further, there is little change in the resistance, which is basically due to the normal resistance of the Josephson junction at $x/a \simeq 17$, until thermal fluctuations lead to further nucleation of vortices, voltage developing across a second Josephson junction at $x/a \simeq 45$, and a second jump in the resistance [see Fig. 2(iii), cor-

responding to point (iii) in Fig. 1(c)]. Increasing the temperature further leads to the formation of additional weak links, resulting in more jumps in the resistance.

Unlike the mechanism suggested in Refs.[7, 8], one does not need to invoke large variations in the coherence length of up to 40% along the sample to quench the SC order. From the data in the first panel of Fig. 2(i) we can estimate the local coherence length using $\xi = \hbar v_F / \pi \Delta$ as varying by no more than $\sim 15\%$ across the sample. In this low dimensional system, small variations in the coherence length are sufficient to induce separation of the system into local SC regions, connected by normal weak-links, due to the increasing importance of thermal fluctuations. On the other hand, the system indeed separates into normal and SC regions, as suggested by Ref.[5], but not due to spontaneous phase separation near a critical point, but due to the interplay of disorder and temperature driven fluctuations. Similar behavior is observed upon keeping the temperature fixed, but increasing the magnetic flux in Fig. 2(iv) [see also point (iv) in Fig. 3(b)]. Here the loss of coherence is not driven by fluctuations, but instead the vortices, induced by the finite magnetic field, disrupt the SC state even at very low temperatures. Nevertheless, we still expect that as a function of flux, the resistance will rise in steps, similar to the steps that emerge with rising temperature. This indeed is borne out by the numerics, as depicted in Fig. 3(b).
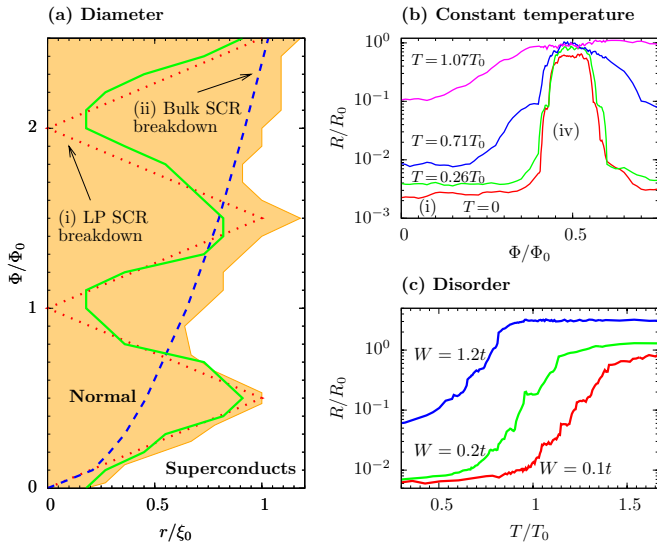
FIG. 3: (Color online) The influence of cylinder geometry on the resistance: (a) The SCR to normal state transition for different cylinder diameters for a $d = 0$ cylinder (green solid) and $d = 0.35r$ (orange shading). The red dotted line (i) shows the mean-field prediction for the LP superconductor-insulator transition, and the blue dashed line (ii) shows the mean-field prediction for the breakdown of superconductivity due to flux penetrating the walls. (b) The variation of resistance with flux for four different cylinder wall thicknesses r. (c) The zero flux superconductor-insulator transition for three levels of disorder.

Furthermore, the lower panel of Fig. 2(iv) shows that for the same system, the breakdown of the SC phase correlations takes place at the same location, $x \simeq 17a$ as it did with increasing temperature in Fig. 2(iv), so pointing toward the same disorder driven transition. The observation that the resistance jumps are almost identical for a longer sample [see Fig. 1(d)], except that there are more of them, further supports the scenario where each step is due to the addition of a single normal weak link.

So far we have concentrated on choosing parameters to best fit the experimental observations. The formalism allows us, naturally, to explore any range of parameters, and make specific predictions. We have already reported in Fig. 1(b) the flux dependence of the resistance for cylinders of different thicknesses. As expected, the thicker the cylinder walls, the larger the magnetic field penetrating the actual sample, and the less periodic the signal is, until at $d \sim 1.05r$, the SC phase

does not reemerge beyond $\Phi = \Phi_0/2$ (the actual value of this thickness may depend on disorder). To study this in more detail Fig. 3(a) depicts the full phase dependence on wall thickness. For a two-dimensional cylinder ($d = 0$) the numerical separatrix between the SC and normal phase deviates from the mean-field expectation $r = \xi_0 \min_n |n + \Phi/\Phi_0|$ [labeled (i)] at small cylinder radii r, due to the fact that in such quasi one-dimensional systems, thermal fluctuations are sufficient to disrupt the SC phase even at zero flux. The filled orange area depicts the SC phase for a finite-thickness cylinder $d = 0.35r$. At small flux we see the same periodic variation as the $d = 0$ cylinder. However, flux penetrating the walls will itself destroy the SC phase along [3] $r = 2\xi_0 \Phi/\Phi_0 \sqrt{1 - T/T_c}$ [labeled (ii)], with ξ_0 the SC coherence length used as a fitting parameter, and so place a bound on the phase boundary.

We have also shown in Fig. 1(d) that the values of the resistance plateaus depend only weakly on the cylinder length, though a longer cylinder is predicted to exhibit more steps. Additionally, Fig. 3(b) demonstrates that one should also see steps in the resistance as a function of flux, for a fixed temperature. Interestingly, these steps persist even above the critical temperature, which is consistent with the picture presented above – the critical temperature corresponds to the formation of the first normal weak link, but additional normal links are formed with increasing flux. Finally, in Fig. 3(c) we plot the variation of resistance for two higher levels of disorder. At higher disorder amplitude the transition temperature decreases, and the normal state resistance increases. Interestingly, the resistance steps persist even for a highly disordered cylinder ($W = 1.2t$) that exhibits a normal resistance at low temperature. This prediction could be readily checked experimentally.

To conclude, we have used *ab initio* simulations to examine recent experiments on the quantum Little Parks effect. The simulations demonstrate step-wise destruction of the SC phase, stemming from phase fluctuations breaking down SC coherence in those parts of the cylinder that have a weaker BCS order parameter, due to disorder. The formalism also allowed specific predictions of further phenomena that could verify this hypothesis.

[1] W.A. Little and R.D. Parks, Phys. Rev. Lett. **9**, 9 (1962).
[2] M. Tinkham, *Introduction to Superconductivity* (McGraw-Hill, New York, 1996), pp. 128130.
[3] P.G. de Gennes, C.R. Acad. Sci. (Paris) Ser. II 292, 279 (1981).
[4] Y. Liu, Y. Zadorozhny, M.M. Rosario, B.Y. Rock, P.T. Carrigan and H. Wang, Science **294**, 2332 (2001).
[5] H. Wang, M.M. Rosario, N.A. Kurz, B.Y. Rock, M. Tian, P.T. Carrigan and Y. Liu, Phys. Rev. Lett. **95**, 197003 (2005).
[6] O. Vafek, M.R. Beasley and S.A. Kivelson, arXiv:0505.688 (2005).
[7] V.H. Dao and L.F. Chibotaru, Phys. Rev. Lett. **101**, 229701 (2008).

[8] V.H. Dao and L.F. Chibotaru, Phys. Rev. B **79**, 134524 (2009).

[9] H. Wang, M.M. Rosario, N.A. Kurz, B.Y. Rock, M. Tian, P.T. Carrigan and Y. Liu, Phys. Rev. Lett. **101**, 229702 (2008).

[10] V.L. Berezinskii, Sov. Phys. JETP **32**, 493 (1971); J.M. Kosterlitz and D.J. Thouless, Journal of Physics C: Solid State Physics, **6**, 1181, (1973).

[11] For a review, see B.I. Halperin, G. Refael and E. Demler, arXiv:1005.3347.

[12] G.J. Conduit and Y. Meir, arXiv:1102.1604.